Fano Lineshape and Phonon Softening in Single Isolated Metallic Carbon Nanotubes

Khoi T. Nguyen, Anshu Gaur, and Moonsub Shim*

Department of Materials Science and Engineering and Frederick Seitz Materials Research Laboratory, University of Illinois at Urbana-Champaign, Urbana, Illinois 61801, USA

(Received 13 December 2006; published 6 April 2007)

Evolution of *G*-band modes of single metallic carbon nanotubes with the Fermi level shift is examined by simultaneous Raman and electron transport studies. Narrow Lorentzian line shape and upshifted frequencies are observed near the van Hove singularities. However, all *G* modes soften and broaden at the band crossing point. The concurrent appearance of an asymmetric Fano line shape at this point indicates that phonon-continuum coupling is intrinsic to single metallic tubes. The apparent Lorentzian line shapes of as-synthesized metallic tubes are induced by O_2 adsorption causing the Fermi level shift.

DOI: 10.1103/PhysRevLett.98.145504 PACS numbers: 63.22.+m, 63.20.Kr, 73.63.Fg, 78.67.Ch

Novel phenomena in 1D continue to be observed in single-walled carbon nanotubes (SWNTs) [1]. In addition, high performance transistors and nanoelectromechanical systems have been demonstrated [2,3]. However, many prospects are hindered by ongoing debates on the inherent properties of SWNTs. A major difficulty arises from all surface-atom makeup of SWNTs where even minute changes in the local environment can alter what appears to be the intrinsic characteristic. One current controversy lies in the Raman *G*-band phonon modes and the nature of electron-phonon coupling in metallic tubes. The lower frequency mode of the *G*-band (G^-) usually exhibits downshifted frequencies and broad line widths [4]. Initially, these features of G^- peak have been attributed to phonon-plasmon coupling based on ensemble measurements [5]. Increasing linewidth and frequency downshift with decreasing average diameter have appeared consistent with the assignment of G^- peak as TO phonons (i.e., the circumferential in-plane mode) and that the broad asymmetric line shape is an intrinsic characteristic [5]. Based on the argument that the available momentum of incident photons for Raman measurements is too small for momentum conservation, coupling to a band of plasmons arising in bundles of SWNTs has been proposed to be the origin of the Fano line shape rather than an intrinsic process in single metallic tubes [6]. Comparisons of Raman measurements on individual bundles and single metallic tubes have led to results where the broad, downshifted, and asymmetric G^- peak disappears upon debundling by mechanical manipulation [7] or by low density chemical vapor deposition (CVD) growth [8]. Narrow linewidths and frequencies similar to semiconducting tubes should then be the intrinsic attributes of metallic tubes. However, the reassignment of G^- peak to LO mode based on dynamic Peierls-like distortion or Kohn anomaly [9–11] contradicts these results. That is, strong electron-phonon coupling damps vibrations of LO mode but not of the circumferential TO mode. Raman measurements on diameter [10] and incident laser energy [12] dependence support this picture. Then, softened and broadened, but not necessarily Fano line shape, only of G^- peak is expected to be the intrinsic attributes of single metallic tubes. Phonon frequencies, linewidths, and line shapes are three key experimentally accessible quantities to measure electron-phonon coupling. Combining Raman studies with electron transport measurements at the single nanotube level can provide new insights, in particular, on how phonon modes evolve with changing of the Fermi level [13,14]. Such measurements are especially important in elucidating what the inherent phonon line shape is and therefore whether or not phenomena such as phonon-plasmon coupling are intrinsic. Here, we report on simultaneous Raman and electrical measurements on single isolated metallic tubes. We observe line broadening, phonon softening, and *asymmetric Fano* line shape of the *G*-band features as the Fermi level passes through the band crossing point halfway between the first pair of van Hove singularities (vHs). At high gate voltages (V_g) where the Fermi level approaches the vHs, Fano line shape converts to Lorentzian in addition to *all* *G*-band modes upshifting to frequencies similar to those of semiconducting tubes. While the softening of G^- peak around the band crossing point is expected based on Kohn anomaly [9–11], the Fano line shape and all *G* peaks softening suggest that a reconsideration of electron-phonon coupling is needed. Furthermore, we point out the importance of the local chemical environment especially with respect to charge transfer from adsorbed molecules. We attribute previous report [8] of vanishing Fano line shape in single metallic tubes to O_2 adsorption induced Fermi level shift.

SWNTs were synthesized by chemical vapor deposition with patterned catalysts [15]. For electrical contacts, Au electrodes with Ti wetting layer were deposited on top of SWNTs grown on heavily doped Si/SiO_2 substrates. Electrochemical gate potential was applied with a nearby electrode, also prepatterned, through a 20 wt% $LiClO_4 \cdot 3H_2O$ in polyethylenimine (Aldrich, low molecular weight) spin coated on top of electrically contacted SWNTs [16]. Thin polymer electrolyte film does not absorb in the wavelength of incident laser. The use of polymer electrolyte as gate

medium provides nearly ideal efficiencies allowing low voltage operation and electrical stability necessary for combined electrical and Raman measurements. Gate leakage current in the voltage range examined is less than 2% of drain-source current at high V_g and ~0.1% at low V_g. Raman spectra were collected with a JY LabRam HR 800 using a 1.96 eV excitation source through a 100× air objective (laser spot diameter ~1 μm). Laser power was kept at or below ~1 mW. No noticeable differences in the Raman spectra between zero bias and the small applied bias of 10 mV across the tube were observed. Baseline correction was carried out by subtracting a spectrum collected ~2 μm away from where the nanotube was located at the same V_g. The baseline does not exhibit any observable V_g dependence. Figure 1 shows D- and G-band regions of the Raman spectrum of a single metallic tube at two different V_g. This tube exhibits a single radial breathing mode (RBM) at 202.3 cm^{-1} with narrow linewidth (FWHM = 6 cm^{-1}) indicating that this is a metallic tube. A diameter of 1.3 nm is obtained from AFM imaging, which is consistent with expected diameter of 1.2 nm based on the RBM frequency. Following Refs. [17–19], we tentatively assign this tube to a (14,2) chiral metallic tube. RBM exhibits a small gate dependent frequency upshift (up to ~3 cm^{-1} within V_g range of ±1 V while FWHM remains $\lesssim$6 cm^{-1}, and a significant intensity decrease as the externally applied V_g moves the Fermi level towards

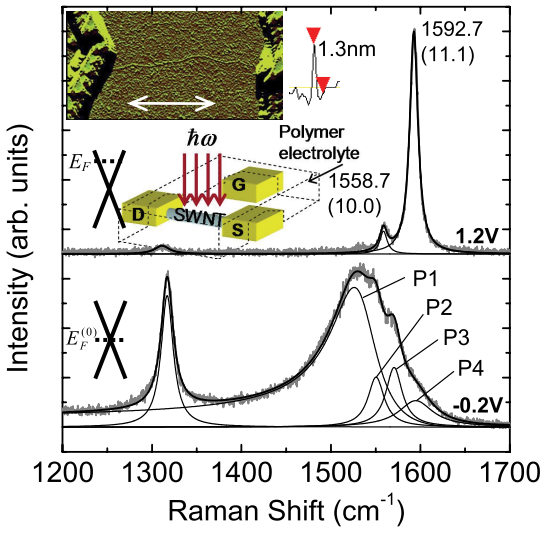

FIG. 1 (color online). Raman spectra of a single isolated metallic tube at the indicated V_g (in bold). Gray lines are the data and the bold black lines are the curve fits as described in the text. Thin lines are components of the curve fit with P1–P4 designated for lower spectrum. Numbers in the upper spectrum correspond to peak position (FWHM) in cm^{-1}. Spectra are offset for clarity. Left two insets are schematic band diagrams indicating Fermi levels. Upper inset is the AFM image (2.5 μm × 5 μm) with height profile. Double headed arrow indicates laser polarization. Middle inset is schematic of the measurement.

either one of the nearest vHs consistent with Ref. [14]. Unlike RBM, G-band exhibits large line shape changes. The upper spectrum at $V_g = 1.2$ V in Fig. 1 is fitted with two Lorentzians for the G-band and one Lorentzian for the D-band. Both features of G-band have frequencies similar to typical single semiconducting tubes of comparable diameter [20,21]. At $V_g = -0.2$ V, there is a minimum in the electrical conductance which indicates that this potential corresponds to the Fermi level being at the band crossing point ($E_F^{(0)}$) between the first pair of vHS. At this V_g corresponding to $E_F^{(0)}$, a broad asymmetric Fano line shape appears. The G-band region of the spectrum at $E_F^{(0)}$ is fitted to three Lorentzians and one Fano line given by $I(\omega) = I_0[1 + q(\omega - \omega_0)/\Gamma]^2/\{1 + [(\omega - \omega_0)/\Gamma]^2\}$, where ω_0 is the spectral position with intensity I_0, q is the measure of phonon coupling to a continuum of states, and Γ is the width. The four features of the G-band are labeled P1 through P4. It is P1 that exhibits asymmetric Fano line shape near $E_F^{(0)}$ but disappears at high V_g. The curve fitting for all data presented here is carried out including the D-band to ensure that changes in the D-band intensity are not mistaken for line shape asymmetry. In contrast to the high V_g all-Lorentzian spectrum, the asymmetric Fano component arising near $E_F^{(0)}$ leads to a nonvanishing intensity well below the D-band region.

In addition to asymmetric line shape, the spectrum at $V_g = -0.2$ V also exhibits broadened linewidths for all G-band modes. The two dominant peaks of the G-band at $V_g = 1.2$ V exhibit very narrow linewidths (FWHM) of ~10 cm^{-1} whereas the corresponding two peaks (P2 and P3) at $V_g = -0.2$ V have FWHMs ~20 cm^{-1}. The asymmetric component P1 also shows about a factor of 2 increase in linewidth near $E_F^{(0)}$ compared to Fermi level near vHs ($2\Gamma = 62$ cm^{-1} at $V_g = -0.2$ V whereas $2\Gamma =$ 28 cm^{-1} and 34 cm^{-1} at $V_g = 0.4$ V and -0.8 V, respectively).

The spectral evolution of another single metallic tube is shown in Fig. 2. RBM is at 203 cm^{-1}, and we therefore expect this tube to have the same chirality as the tube shown in Fig. 1. In Fig. 2(a), gradual narrowing of the broad asymmetric Fano line shape and frequency upshift are observed from $V_g = 0$ V to 0.9 V. The negative V_g region is shown in Fig. 2(b). Similar change in the loss of Fano component P1 as in the positive gate voltage region is observed but to a lesser extent. Spectra in Figs. 2(a) and 2(b) are fitted in the same manner as the lower spectrum in Fig. 1. For the metallic tube shown in Fig. 2, P1 persists within our V_g range of ±1 V, but P4 disappears for $V_g >$ 0.7 V. The asymmetry of P1 peak starts to disappear at $V_g \sim 0.7$ V, and the spectra can be fit equally well with either Fano or Lorentzian line shape for $V_g > 0.7$ V.

In Fig. 2(b), the Raman spectrum prior to polymer electrolyte deposition is also shown. Notice that line

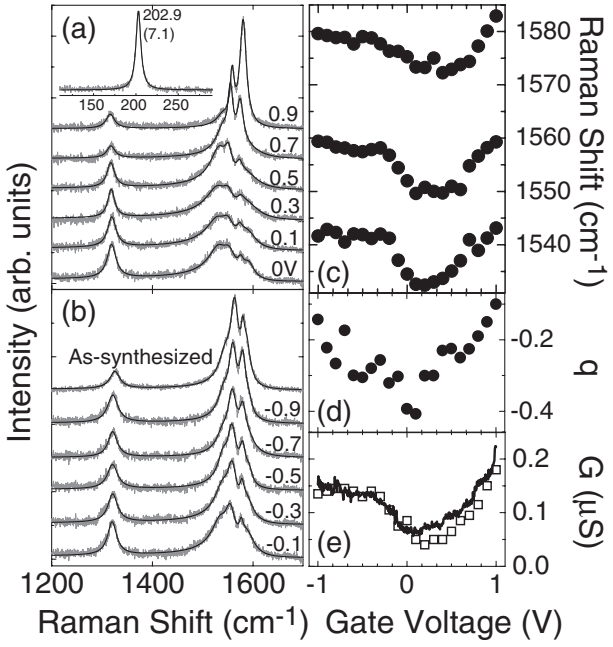

FIG. 2. Raman spectra of a metallic tube at positive (a) and negative (b) V_g swept from -1 to $+1$ V at 0.1 V step. Only spectra at 0.2 V intervals and at 0 V are shown and offset for clarity. Top spectrum in (b) and RBM in inset of (a) correspond to the same tube prior to polymer electrolyte deposition without applied V_g. Peak position (FWHM) for RBM is indicated. V_g dependence of frequency shifts (c) and Fano line coupling parameter q for P1 (d) compared with electrical conductance (e). Open squares are conductance during Raman measurements and line is conductance before in the dark.

shapes, widths, and frequencies of this tube as-synthesized all resemble spectra at $V_g < -0.5$ V. There are two important implications of these observations. First is that the adsorption of polymer electrolyte does not have any noticeable effects other than shifting the Fermi level as expected from Ref. [22]. The second implication is that the Fermi level of the metallic tube in air ambient lies several hundred meV below $E_F^{(0)}$. While debates over whether or not charge transfer occurs from O_2 have mainly focused on semiconducting tubes [23–27], metallic tubes with finite density of states around $E_F^{(0)}$ should be much more prone to charge transfer. These changes in G-band line shape imply electron transfer to O_2.

Figures 2(c)–2(e) compare the V_g dependent frequency shifts of three main G-band peaks and the coupling parameter q with the electrical conductance. Conductance before (in the dark) and during the Raman measurements are shown together indicating that the low laser intensities used here do not have any significant effect. Considering that polymer electrolyte gating leads to nearly ideal gate efficiencies and that the nanotube is resonant with 1.96 eV incident laser, the increase in the conductance at positive and negative V_g should correspond to increasing electronic density of states as the Fermi level nears the first pair of vHs. The conductance minimum at $V_g \sim 0.2$ V then corresponds to the Fermi level at $E_F^{(0)}$.

In Raman measurements during electrochemical doping of SWNT "mats," softening of two lower frequency modes of G-band near $E_F^{(0)}$ has been reported [28]. The highest frequency mode, on the other hand, exhibits a monotonic downshift with increasing Fermi level. Since the two lower frequency modes are expected to be LO modes, these observations have been interpreted to be consistent with the dynamic Peierls-like distortion in metallic tubes as predicted in Ref. [9]. Many factors including the overlapping G-band frequencies of metallic and semiconducting tubes and bundling effects can complicate the situation with SWNT mats. The most prominent effect on the Raman spectrum of a single isolated metallic tube as shown in Fig. 2(c) is the softening of *all* G-band peaks coincident with the conductance minimum. Concurrent line broadening with softening suggests that electron-phonon coupling, whether it involves plasmons or not, becomes stronger near $E_F^{(0)}$ for all modes.

Figure 2(d) shows the coupling parameter q obtained from curve fitting. Much like the changes in phonon frequencies, the correlation with conductance is notable. As the Fermi level moves away from $E_F^{(0)}$ towards either one of the vHs, increasing electronic density of states should change the plasmon frequency and may lead to decoupling of the phonon transitions to plasmons. While these results are consistent with phonon-plasmon coupling effects, other factors need to be carefully examined.

Two immediate extrinsic factors are contributions from the metal electrodes and the ambient molecular adsorption. Figure 3 shows the changes in the Raman spectrum of a single isolated metallic tube without any electrical contacts upon Ar annealing and subsequent O_2 exposure. The CVD growth is the last step taken for this sample, and therefore only the ambient molecular adsorption rather than any post-synthesis fabrication process should contribute to what we observe. When the Ar annealed tube is exposed to O_2, P1 upshifts from 1545 to 1550 cm^{-1}, and the linewidth 2Γ narrows from 55 to 32 cm^{-1}. The absolute value of q also decreases from 0.29 to 0.07. Exposure to O_2 leads to Raman features very similar to those of as-synthesized tube that has been exposed to air. These changes in the G-band upon O_2 exposure are essentially identical to the changes observed in shifting the Fermi level with external V_g from near $E_F^{(0)}$ to a few hundred meV below $E_F^{(0)}$. These results suggest that O_2 adsorption leads to electron transfer from metallic tubes and that the metal leads do not contribute to the appearance of the Fano line shape.

We make a final comment on the apparent correlation between the D-band intensity and the changes in the G-band. Both metallic tubes shown in Figs. 1 and 2 exhibit

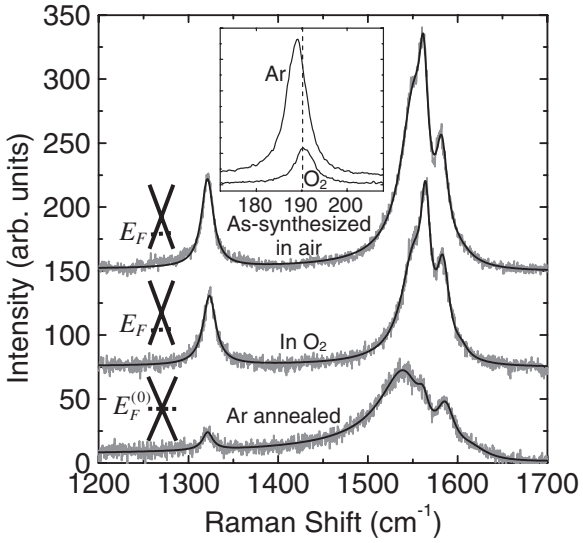

FIG. 3. Raman spectra of a metallic tube under indicated conditions. Annealing was carried out at 450 °C for 15 min under 100 cm^3/min Ar flow. Ar and O_2 used are 99.95%. Left insets show schematics of band diagrams with corresponding Fermi levels. Upper inset is RBM showing decreased intensity and slight upshift under O_2 similar to negative V_g effects.

enhanced D-band intensity as the Fermi level passes through $E_F^{(0)}$ where line shape asymmetry, broadening, and softening are the most pronounced. Then disorder scattering may provide the necessary momentum for discrete phonon-plasmon coupling even in single tubes. However, when the asymmetric Fano line shape is taken into account, the integrated D/G intensity ratio remains constant within V_g range studied here providing another indication of Fano line shape being an intrinsic attribute of metallic tubes. Since the degree of disorder does not change with gating while the Fano component does, disorder scattering is not likely to be contributing to phonon-continuum coupling. Furthermore, there is an order of magnitude *decrease* in the D/G ratio as well as the D-band intensity (i.e., decrease in the actual tube disorder) while broadening, softening, and asymmetry of the G-band are most pronounced after thermal desorption of O_2 in Fig. 3. These observations indicate that Fano line shape is independent of induced disorder (but strongly affected by charge transfer) and further support the asymmetric line shape being an intrinsic attribute of metallic tubes.

In conclusion, we have shown that Fano line shape is inherent to single metallic nanotubes and that the Fermi level shift towards vHs changes the line shape to Lorentzian. Adsorption of O_2 has the same effect on G-band as lowering of the Fermi level and can explain why Lorentzian line shape was previously reported [8] in single metallic tubes. Electron-phonon coupling in nanotube 1D conductors should include phonon-continuum coupling in addition to phonon softening via Kohn anomaly.

This material is based upon work supported by NSF (Grant Nos. CCF-0506660 and DMR-0348585). Atomic force microscopy was carried out in the Center for Microanalysis of Materials, University of Illinois at Urbana-Champaign, which is partially supported by the U.S. Department of Energy under Grant No. DEFG02-91-ER45439.

*Electronic address: mshim@uiuc.edu

[1] S. Ilani *et al.*, Nature Phys. **2**, 687 (2006).
[2] X. J. Zhou *et al.*, Phys. Rev. Lett. **95**, 146805 (2005).
[3] H. B. Peng *et al.*, Phys. Rev. Lett. **97**, 087203 (2006).
[4] M. S. Dresselhaus *et al.*, Phys. Rep. **409**, 47 (2005).
[5] S. D. M. Brown *et al.*, Phys. Rev. B **63**, 155414 (2001).
[6] K. Kempa, Phys. Rev. B **66**, 195406 (2002).
[7] C. Jiang *et al.*, Phys. Rev. B **66**, 161404 (2002).
[8] M. Paillet *et al.*, Phys. Rev. Lett. **94**, 237401 (2005).
[9] O. Dubay, G. Kresse, and H. Kuzmany, Phys. Rev. Lett. **88**, 235506 (2002).
[10] M. Lazzeri *et al.*, Phys. Rev. B **73**, 155426 (2006).
[11] V. N. Popov and P. Lambin, Phys. Rev. B **73**, 085407 (2006).
[12] J. Maultzsch *et al.*, Phys. Rev. Lett. **91**, 087402 (2003).
[13] S. B. Cronin *et al.*, Appl. Phys. Lett. **84**, 2052 (2004).
[14] Z. Wang *et al.*, Phys. Rev. Lett. **96**, 047403 (2006).
[15] J. Kong *et al.*, Nature (London) **395**, 878 (1998).
[16] G. P. Siddons *et al.*, Nano Lett. **4**, 927 (2004).
[17] J. Maultzsch *et al.*, Phys. Rev. B **72**, 205438 (2005).
[18] J. C. Meyer *et al.*, Phys. Rev. Lett. **95**, 217401 (2005).
[19] A. Jorio *et al.*, Phys. Status Solidi B **243**, 3117 (2006).
[20] A. Jorio *et al.*, Phys. Rev. Lett. **90**, 107403 (2003).
[21] M. Paillet *et al.*, Phys. Rev. Lett. **96**, 257401 (2006).
[22] M. Shim *et al.*, J. Am. Chem. Soc. **128**, 7522 (2006).
[23] M. Shim *et al.*, Phys. Rev. B **71**, 205411 (2005).
[24] G. Dukovic *et al.*, J. Am. Chem. Soc. **126**, 15269 (2004).
[25] S. Heinze *et al.*, Phys. Rev. Lett. **89**, 106801 (2002).
[26] P. G. Collins *et al.*, Science **287**, 1801 (2000).
[27] G. U. Sumanasekera *et al.*, Phys. Rev. Lett. **85**, 1096 (2000).
[28] P. M. Rafailov *et al.*, Phys. Rev. B **72** 045411 (2005).